



HAL
open science

Analysis of the effects of partial discharges in a power cable for aeronautical applications

Vladimir Pineda Bonilla, Riantsoa Rabemarolahy, Françoise Foray, Michael J Kirkpatrick, Philippe Molinié, Emmanuel Odic

► **To cite this version:**

Vladimir Pineda Bonilla, Riantsoa Rabemarolahy, Françoise Foray, Michael J Kirkpatrick, Philippe Molinié, et al.. Analysis of the effects of partial discharges in a power cable for aeronautical applications. International Conference on More Electrical Aircraft Towards cleaner aviation 2024, Feb 2024, Toulouse, France. hal-04506036

HAL Id: hal-04506036

<https://hal.science/hal-04506036v1>

Submitted on 15 Mar 2024

HAL is a multi-disciplinary open access archive for the deposit and dissemination of scientific research documents, whether they are published or not. The documents may come from teaching and research institutions in France or abroad, or from public or private research centers.

L'archive ouverte pluridisciplinaire **HAL**, est destinée au dépôt et à la diffusion de documents scientifiques de niveau recherche, publiés ou non, émanant des établissements d'enseignement et de recherche français ou étrangers, des laboratoires publics ou privés.

Analysis of the effects of partial discharges in a power cable for aeronautical applications

Vladimir Pineda Bonilla (1)(2), Riantsoa Rabemarahy (2), Françoise Foray (2), Michael J. Kirkpatrick (1), Philippe Molinié (1), Emmanuel Odic (1)

1: Laboratoire de Génie Électrique et Électronique de Paris (GeePs -UMR8507 CNRS, CentraleSupélec, Université Paris-Saclay, Sorbonne Université) Gif-sur-Yvette, France, email :
firstname.lastname@centralesupelec.fr, except mike.kirkpatrick@centralesupelec.fr

2 : Airbus Helicopters, Marignane, France, email: firstname.lastname@airbus.com, except vladimir.ricardo-pineda-bonilla@airbus.com

Vladimir Ricardo PINEDA BONILLA is a member of the AIRBUS HELICOPTERS personnel in the context of an industrial collaboration CIFRE and is affiliated to UNIVERSITE PARIS-SACLAY as a PHD student, in the context of a collaboration agreement between AIRBUS HELICOPTERS, CENTRALESUPELEC and SORBONNE UNIVERSITE.

1. Abstract

The objective of this study was to investigate the behavior of the electrical insulation system of a power cable in the presence of partial discharges (PDs). The cable was taped DH gauge 2 with PTFE insulation, currently used in aircraft. A PD aging chamber has been designed and constructed. The cable specimens were partially covered with grounded shielding braid. Thus, when a voltage exceeding the system partial discharge inception voltage (PDIV) was applied to the center conductor (~30 kHz AC sinusoidal voltage), the insulation system was subjected to partial discharges over a cable length delimited by the dimensions of the ground braid. Accelerated ageing was carried out at room temperature and atmospheric pressure. The conditions for the presence of external discharges (discharges initiated at the ground braid conductors in contact with the outer insulating face of the cable) and internal discharges (discharges initiated in the internal cavities of the insulation at the peripheral strands of the conductor) were identified based on the experimental conditions (amplitude of the applied voltage, geometry of the ground braid). For each aging condition, the mean power dissipated in the discharge was measured, and the delay to failure noted. During aging certain specimens, PDIV was also measured.

Introduction

With the prospect of more electric aircraft (MEA) and all-electric aircraft (AEA), the increase in on-board electrical power results in a rise in on-board network voltage. This rise in voltage is becoming a major constraint for electrical systems, particularly for electrical insulation systems which are not designed for these "high voltages". As a result, the risk of partial discharge (PD) increases, which in the medium to long term can lead to accelerated ageing of solid insulation systems and ultimately to failure (dielectric breakdown).

In this context, the power cable is a component that needs to be characterized with respect to these new voltage constraints under varied and sometimes severe environmental conditions [1]. Previous work [2] has highlighted the effect of accelerated thermal ageing (several months at 240°C) on partial discharge inception voltage (PDIV). In addition, a differentiation was established between internal PD (discharges initiated in the internal cavities of the insulation at the

peripheral strands of the conductor) and external PD (discharges initiated at the ground braid conductors in contact with the outer insulating face of the cable) [2]. A 25% to 40% drop in PDIV was observed after prolonged thermal ageing (more than 9000 hours) [2]. However, the impact of this type of discharge has not been investigated in depth with regard to failure [3]. In fact, internal and external discharges occur at different voltages and in different locations in the cable, so their effects need to be analyzed separately.

It is well known that the presence of partial discharges in a solid insulation system can have harmful effects in a very short time compared with the operating life of the component [4]. However, the dynamics and severity of these effects can vary greatly from one system to another. Specific studies therefore need to be carried out [5].

For all these reasons, a high-voltage, medium frequency (~30 kHz) test campaign was conducted to measure the effects of partial discharges in cables. Particular attention was paid to the evolution of the

PDIV during combined ageing and to identifying the type of partial discharge.

1. Experimental setup

1.1. Test setup

A partial discharge ageing chamber was designed and built for this study. The purpose of this air-tight chamber was to contain cable samples whose solid insulation was to be subjected to partial discharges. For this purpose, the chamber was fitted with a high-voltage feedthrough and a ground connection that enabled an electric field to be imposed on the cable insulation (Figure 1). A constant air flow (RH < 5% Vol. at room temperature and 1 L/min) was imposed at atmospheric pressure through the chamber to prevent the accumulation of ozone produced by the electrical discharges [6].

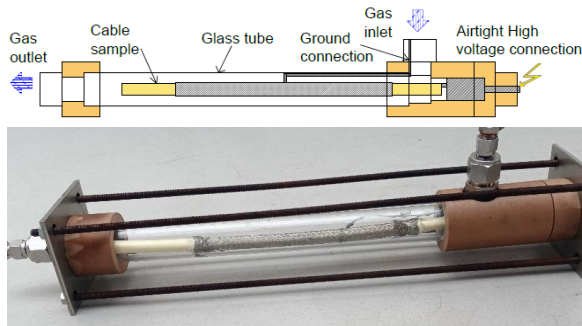


Figure 1 Diagram and picture of the chamber containing a sample.

1.2. Sample preparation

The samples were 30 cm sections of cable (taped DH gauge 2 with PTFE insulation). A connector was fitted to one of the conducting ends so allowing voltage to be imposed to the cable conductor. The cable sample was partially covered with grounded shielding braid over a length of 20 cm. The metallic braid was stretched as far as possible to minimize the air space with the cable external insulation, then fixed. The ends of the braid were retracted, and the junction with the air and insulation was coated with insulating silicone grease to prevent surface discharges in this area where the geometry creates a higher electric field concentration (Figure 2). This leads to PDs appearing only in the rest of the metallic braid area where a more homogeneous electric field is present and thus to apply the same condition to the whole sample.

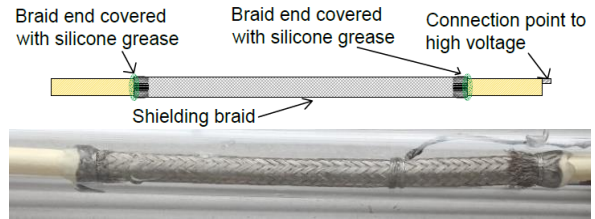


Figure 2 Diagram and picture of a sample.

1.3. Preliminary tests

Firstly, the external and internal PDIV were measured at 50 Hz using a partial discharge analyzer (Omicron MPD-600). The values obtained correspond to an average of the values measured during 9 successive experiments.

The external PDIV was measured using the braid as counter-electrode, with the treatment of its ends described in the previous section. For internal PDIV measurements, the procedure was based on eliminating external discharges by 2 different methods (Figure 3): (i) by immersing the cable (the part under the braid) in insulating oil (as already practiced in other works [2] [3]), (ii) by replacing the braid with a copper foil glued to the surface of the cable (the ends of the copper electrode being protected by silicone grease, thus avoiding surface discharges to occur).

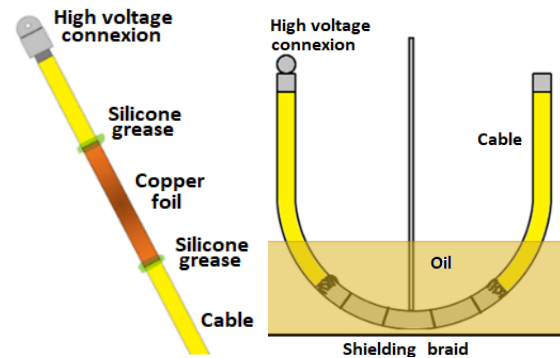


Figure 3 Two ways of measuring the internal PDIV: left - measurement with copper counter-electrode. Right - measurement with dielectric oil.

2. Experimental procedure

Two types of tests were carried out: delay to failure and evolution of the PDIV during ageing. For ageing under partial discharges, a 30 kHz sinusoidal voltage was applied to the cable conductor. Voltage was measured at the high-voltage feedthrough of the enclosure using a Tektronix P6015 A probe (1:1000 ratio, 75 MHz bandwidth). Current was measured at the grounding

conductor of the braid using a Tektronix CT2 probe (1 mV/mA ratio, 1.2 kHz-200 MHz bandwidth). Current and voltage signals were acquired using a digital oscilloscope (Tektronix MSO54, 500 MHz, 6.25 GS/s). The average value (calculated over an integer number of periods of the voltage signal) of the instantaneous product of the voltage and current signals corresponds to the mean discharge power. The values retained for PDIV correspond to 5 successive measurements using the partial discharge analyzer.

2.1. Delay to failure

Voltage (of fixed amplitude and frequency) was applied to the cable conductor until the insulation system failed (solid insulation system breakdown). The time between voltage application and failure was measured. For each voltage level, 7 specimens were tested.

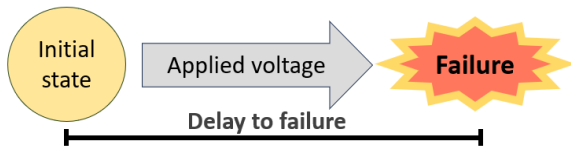


Figure 4 Delay to failure test.

2.2. PDIV evolution:

The PDIV of an unaged specimen was measured. High voltage at medium frequency (~30 kHz) was applied to the cable conductor for a certain period of time, after which ageing was stopped. The PDIV was then measured again. The ageing process was then repeated under the same conditions and for the same period of time. The ageing and PDIV measurement phases were repeated until the system failed.

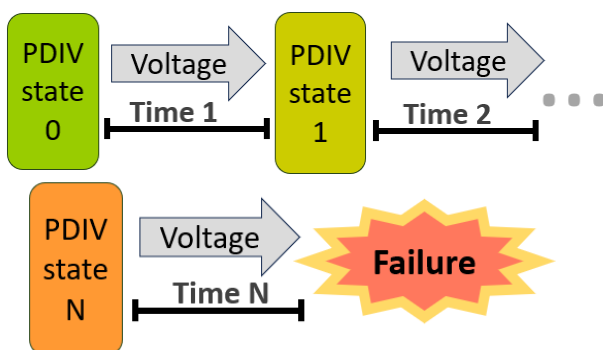


Figure 5 PDIV evolution test.

3. Results

3.1. Preliminary measurements

First, the PDIV of unaged samples prepared as described in section 1.2 was measured for three pressure levels: 200 mbar, 600 mbar and 1000 mbar.

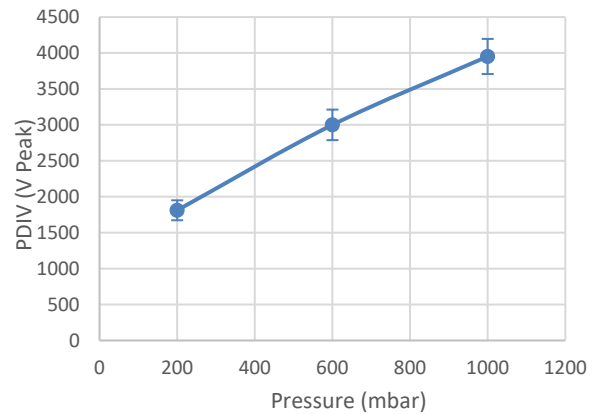


Figure 6 PDIV of unaged samples. Each point is the average of measurements made on three different specimens with five repetitions for each sample. Error bars are the standard deviation of the measurements.

PDIV was seen to increase with pressure (Figure 6) which is an expected behavior [7]. Dependence with air pressure confirms that the measured partial discharges are not localized inside the insulation system of the cable (e.g. closed voids) but in areas open to the surrounding atmosphere, either in internal cavities of the insulation at the peripheral strands of the conductor, or at the interface between the braid and the outer face of the insulation. A further increase in voltage level produces visible light emission in the gaps between the braid strands and the cable's external insulation (Figure 7), thus confirming the location of the measured partial discharges.



Figure 7 Filamentary discharges homogeneously distributed in the air gaps at the braid / cable insulation interface.

In addition, the internal PDIV was measured as described in section 1.3.

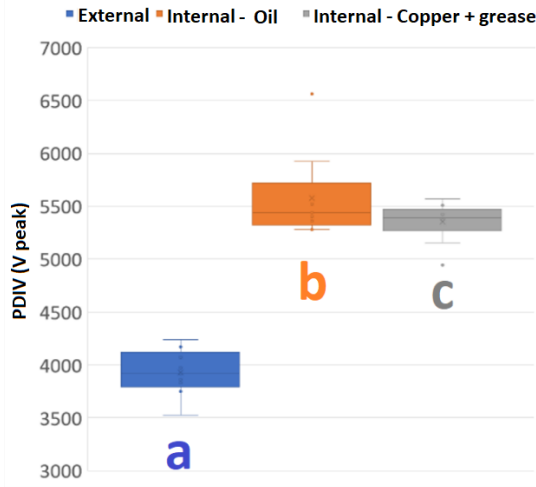


Figure 8 PDIV at 1000 mbar for a same cable specimen: a) External PDs (blue); b) Internal PDs – braid immersed in isolating oil (orange); c) Internal PDs – copper foil protected with silicone grease (gray). Each box is calculated based on 9 measurements. Lower whiskers contain the first quartile, the boxes contain second and third quartile, and the higher whiskers contain the fourth quartile.

Similar PDIV values were obtained with the braid immersed in insulating oil and with the copper and grease, indicating that this counter-electrode has eliminated the external discharges (Figure 8). In addition, it is also verified that external discharges appear at lower voltages than internal discharges (which is in line with previous results [2]).

3.2. PDIV Evolution

Voltage levels and ageing cycle times at atmospheric pressure are shown in **Table 1**. Between each ageing cycle, pauses of 18 hours were made during which the PDIV was measured. Relatively short cycle times were chosen to ensure that at least one middle state could be measured. Each experiment consisted of cycles and pauses (during which PDIV were measured) continuously chained until the breakdown of the cable. The effect of the pauses on the delay to breakdown times of these samples will be discussed in the next section.

Table 1 Voltage levels and cycle times for the PDIV evolution experiments.

Tension (V peak)	% of initial external PDIV	% of initial internal PDIV	Ageing cycle time (minutes)	Number of complete cycles
5000	125%	90%	90	2
5750	144%	104%	10	4
6500	163%	117%	10	1

A first observation is that as the ageing progressed, an observable degradation in the surface of the cable appeared and became more and more evident (Figure 9).



Figure 9 Unaged cable (left) and aged cable after breakdown (right). Note in the aged cable a degradation in the form of brand prints and a perforation resulting from the breakdown.

5000 V Peak:

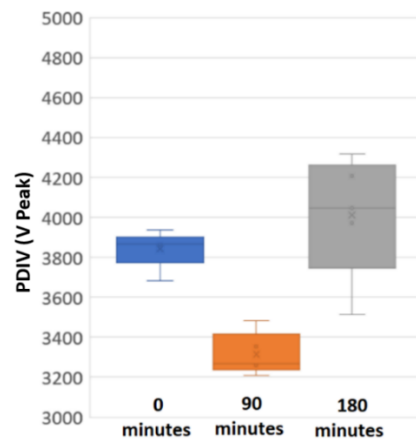


Figure 10 PDIV evolution under a 5000 V peak ageing. Each boxplot includes 5 successive measurements.

5750 V Peak:

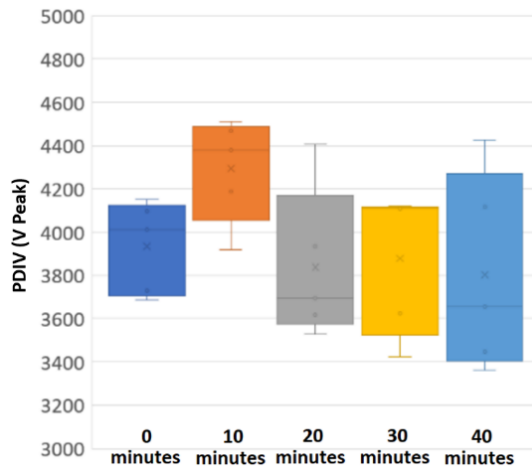


Figure 11 PDIV evolution under a 5750 V peak ageing. Each boxplot includes 5 successive measurements.

6500 V peak

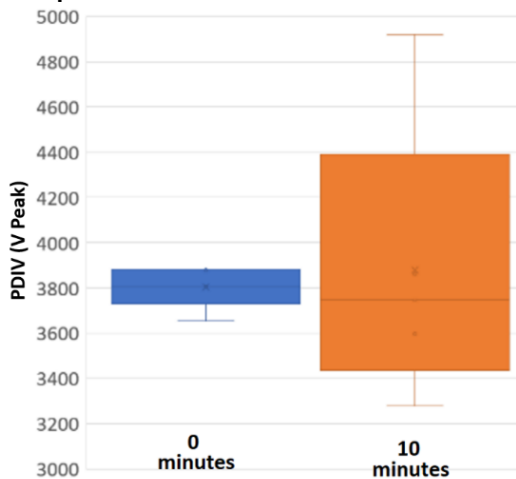


Figure 12 PDIV evolution under a 6500 V peak ageing. Each boxplot includes 5 successive measurements.

For the three voltage values (Figures 10-12), PDIV in the last middle state was very similar to PDIV at initial state (unaged). Some variation was seen for the first middle state showing a decrease at 5 kV and an increase at 5.75 kV.

A PDIV evolution study with internal partial discharges in oil was conducted as well. A voltage of 6,5 kV peak was used with cycles of 90 minutes and measurements of internal PDIV during the pauses. Nevertheless, after 450 minutes of treatment, no evolution of internal PDIV was observed and there was no breakdown.

3.3. Delay to failure

For the delay-to-failure tests, the voltages shown in **Table 2** were used. For each voltage level, 7 different cable specimens were tested.

Table 2 Voltages used for delay-to-failure measurements. For all tests, the frequency of the applied voltage is 30 kHz.

Tension (V peak)	% of initial external PDIV	% of initial internal PDIV
4400	110%	80%
5250	131%	95%
5500	138%	100%
5750	144%	104%
6500	163%	117%

In all cases, the samples were subjected to external discharges, and for the highest voltages (above 5.5 kV) to internal discharges as well.

The measured delay-to-failure times are shown in **Figure 13**. For each voltage level, 7 samples were aged uninterruptedly. Additionally, the cumulated delay to failure times for two samples treated by cycles (i.e. with ageing interruptions) are shown as well (in green). As expected, delay to failure time decreases with increasing voltage. Note that the dispersion of the measured times also falls significantly with voltage. Furthermore, cumulated delays to failure of samples treated by cycles are close to delays to failure of uninterruptedly aged samples.

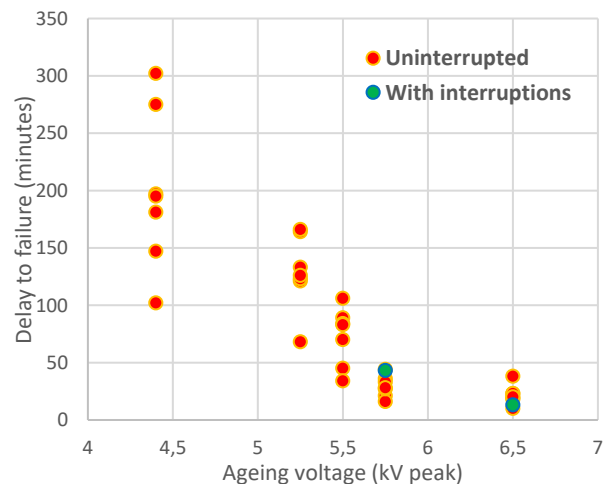


Figure 13 Delay time to failure as a function of applied voltage (30 kHz frequency). Each point is a measurement. At 4.4 kV, 5.25 kV and 5.5 kV only external discharges are present; at 5.75 kV and 6.5 kV, both internal and external discharges are present.

A Weibull analysis was applied to the delay to failure data obtaining the following Probability Density Functions and Cumulative Distribution Functions.

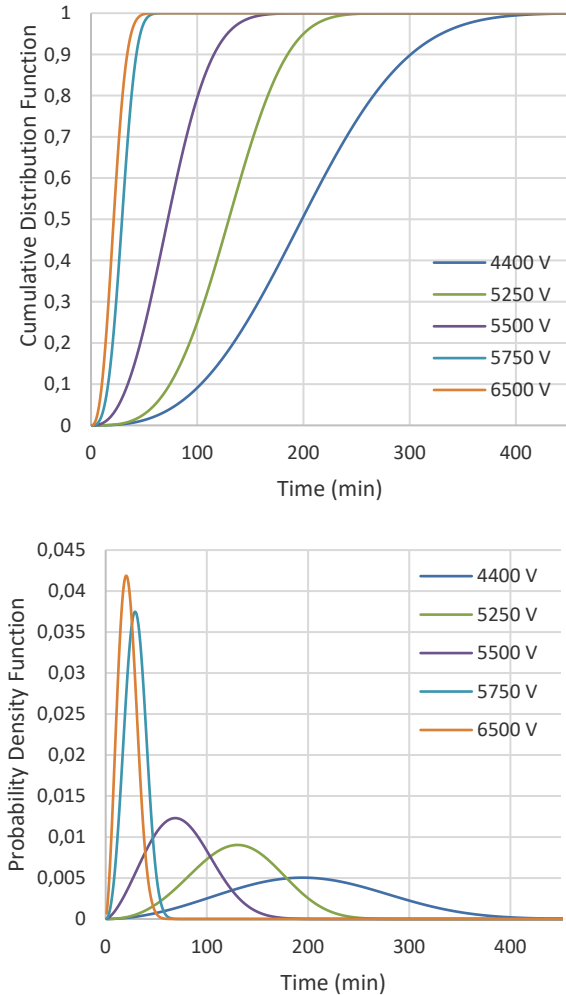


Figure 14 Cumulative Distribution Functions (top) and Probability Density Functions (bottom) for the delay to breakdown data.

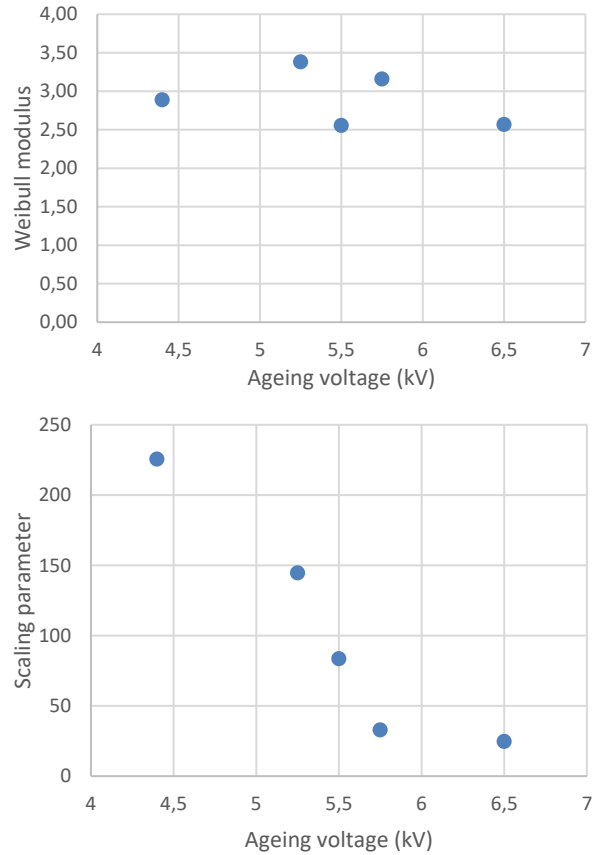


Figure 15 Weibull modulus (top) and Scaling parameter (bottom) of the delay to breakdown data.

Weibull moduli take values between 2.5 and 3.4 (top of Figure 15) which indicates a wear-out failure kind of behavior [8]. The scaling parameter (bottom of Figure 15) decreases with increasing voltage in an almost linear way between 4,4kV and 5,75 kV but after 5,75 kV, the scaling parameter changes very little.

Finally, mean power dissipated in partial discharges discharge increased linearly with applied voltage amplitude for the whole range included in this study (Figure 16). Mean discharge power was seen to vary from one specimen to another but was stable during the ageing for all cases even minutes before breakdown.

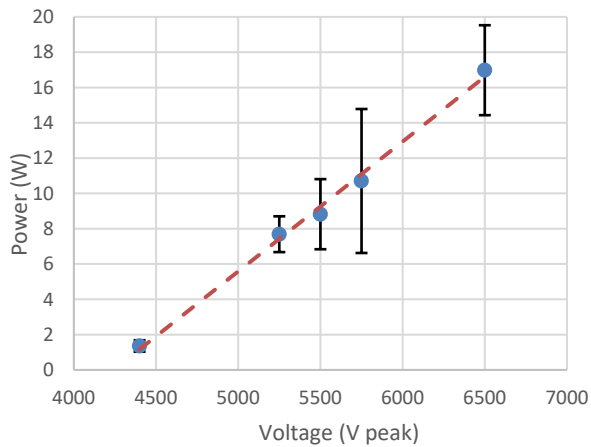


Figure 16 Partial discharge mean power as a function of ageing voltage from the delay to breakdown data.

Concluding remarks

The aim of all the tests carried out was to study, from a macroscopic point of view, the effect of the presence of partial discharges at the level of a component (cable) of the power network. The amplitude and voltage profile were chosen so that, on the one hand, these effects could be observed over a reasonable period of time, and, on the other hand, the conditions of a load supplied by a PWM-controlled power converter could be taken into account (justifying the choice of a 30 kHz frequency). However, it should be noted that the ageing under discharge was only carried out at atmospheric pressure and room temperature, and that the cable under test was not designed to be operated under such voltage conditions.

Both internal and external partial discharges in the cable were considered. The first important finding is that internal discharges have a small effect on cables compared with external discharges. Ageing under internal discharges alone produced no observable effect (on the time scale considered) on the cables, either in terms of PDIV evolution or in terms of premature failure. Furthermore, the mean power dissipated in PDs during ageing increased almost linearly with voltage, independently of the presence or absence of internal discharges. This linear dependency of discharge power as a function of applied voltage was expected as it has been observed in dielectric barrier systems (DBD) which are very similar to the DH2 samples [9]. Drawing a parallel between the cables and DBD systems, a possible explanation is that for lower voltages only a fraction of the total available surface area is covered by discharges and this area increases with an increase in

voltage, thus producing an increase in dissipated power. Once the voltage level is high enough to cover the whole available surface area, the increase in the dissipated power is caused by an increase in both surface density of elementary discharges and intensity of each individual elementary discharge.

As observed in **Figure 13** and in the Weibull analysis, the delay to failure measured have a high dispersion for the lower voltages; this dispersion is strongly reduced for higher voltage. The relative unvarying values of the Weibull modulus suggest that the general distribution of the delays to failure does not change significantly as the ageing voltage increases. On the other hand, the evolution of the scaling parameter with ageing voltage indicates an almost linear decrease in the delays to breakdown until a critical value of around 5,75 kV above which these delays to failure decrease more slowly.

This results together with the PD power measurements suggest that for the lower voltage levels, only a few locations are submitted to PDS and, depending on whether these regions happen to have small fabrication defects or irregularities, the delay to failure can be longer or shorter and the results are more disperse. As the ageing voltage increases, larger areas of the cable are aged and the probability of more vulnerable areas being aged increases, producing shorter delays to failure and less disperse results. If a critical voltage value is applied, the whole available surface area is aged and thus the most vulnerable parts of the cable will always be exposed to some degree of partial discharges. This situation results in shorter times and lower dispersion. Above this critical voltage value, the decrease in the delays to failure is driven by an increase in the intensity of the discharges, which has a lower general effect and for this reason the delays to failure decrease less and less with an increase in voltage. All in all, these results suggest a strongly stochastic failure mechanism where small differences in braid or cable quality can have a significant effect, especially for lower voltages.

Another notable result is that the samples whose treatments were interrupted to measure the PDIV showed delays to failure similar to those obtained during uninterrupted treatments. This result, and the fact that the last treatment time was always very short compared with the total time to failure, show that the effects of treatments with partial discharges are irreversible.

Finally, PDIV does not seem to vary significantly during ageing under partial discharges. Even a few minutes before failure, the PDIV value remained stable. Thus, the progressive degradation of the solid insulation system does not appear to modify, on the time scales considered, the geometric and dielectric characteristics of the solid insulation system that can be detected through PDIV measurement alone. Other characterization methods are required and are the subject of ongoing work.

Electrost., vol. 69, n.º 4, pp. 302-312, ago. 2011, doi: 10.1016/j.elstat.2011.04.007.

References

- [1] G. Lopez, «High-Performance Polymers for Aeronautic Wires Insulation: Current Uses and Future Prospects», *Recent Prog. Mater.*, vol. 3, n.º 1, Art. n.º 1, feb. 2021, doi: 10.21926/rpm.2101005.
- [2] M. Karadjian, «Endurance et tenue diélectrique de l'isolation de câbles électriques pour l'aéronautique», Gif-sur-Yvette, 18 de diciembre de 2018.
- [3] M. Karadjian, N. Imbert, C. Munier, M. Kirkpatrick, y E. Odic, «Partial Discharge Detection in an Aeronautical Power Cable», en *2018 AIAA/IEEE Electric Aircraft Technologies Symposium*, Cincinnati, Ohio: American Institute of Aeronautics and Astronautics, jul. 2018. doi: 10.2514/6.2018-5033.
- [4] G. C. Montanari, P. Seri, S. F. Bononi, y M. Albertini, «Partial Discharge Behavior and Accelerated Aging Upon Repetitive DC Cable Energization and Voltage Supply Polarity Inversion», *IEEE Trans. Power Deliv.*, vol. 36, n.º 2, pp. 578-586, abr. 2021, doi: 10.1109/TPWRD.2020.2984766.
- [5] J. Rivenc *et al.*, «Analysis of standard parts aging under partial discharges for airborne applications», en *2022 IEEE Transportation Electrification Conference & Expo (ITEC)*, Anaheim, CA, USA: IEEE, jun. 2022, pp. 902-907. doi: 10.1109/ITEC53557.2022.9814068.
- [6] P. Yao, H. Zheng, X. S. Yao, y Z. Ding, «A Method of Monitoring Partial Discharge in Switchgear Based on Ozone Concentration», *IEEE Trans. Plasma Sci.*, vol. 47, n.º 1, pp. 654-660, ene. 2019, doi: 10.1109/TPS.2018.2876412.
- [7] A. N. Esfahani, S. Shahabi, G. Stone, y B. Kordi, «Investigation of Corona Partial Discharge Characteristics Under Variable Frequency and Air Pressure», en *2018 IEEE Electrical Insulation Conference (EIC)*, San Antonio, TX: IEEE, jun. 2018, pp. 31-34. doi: 10.1109/EIC.2018.8481047.
- [8] A. Kızılersü, M. Kreer, y A. W. Thomas, «The Weibull Distribution», *Significance*, vol. 15, n.º 2, pp. 10-11, abr. 2018, doi: 10.1111/j.1740-9713.2018.01123.x.
- [9] J. Kriegseis, B. Möller, S. Grundmann, y C. Tropea, «Capacitance and power consumption quantification of dielectric barrier discharge (DBD) plasma actuators», *J.*